A brightening coronal loop observed by TRACE: I. Morphology and evolution

F. Reale, G. Peres, S. Serio[1]
Dip. di Scienze Fisiche & Astronomiche – Sez. di Astronomia – Univ. di Palermo, Piazza del Parlamento 1, I–90134 Palermo, Italy
[1] *Osservatorio Astronomico, Piazza del Parlamento 1, I–90134 Palermo, Italy*

E. E. DeLuca, L. Golub
Smithsonian Astrophysical Observatory, 60 Garden Street, Cambridge, MA 02138, USA

ABSTRACT

We analyze the transient brightening of a solar coronal loop observed, at high time cadence (30 sec) and spatial resolution (0.5" pixel size), with TRACE in the 171 Å band on June 26, 1998. The loop, located in AR 8253, is $\approx 10^{10}$ cm long and inclined with respect to the vertical to the solar surface. Its geometry and shape do not change significantly during the brightening, which lasts for ~ 2 hours and is preceded by highly dynamic events in nearby and perhaps interacting loops. The loop footpoints brighten first; after ~ 10 min, moving brightness fronts rise initially from the northern footpoint, and after further ~ 7 min from the southern one, at an apparent speed ~ 100 km/s, the whole loop becoming clearly visible afterwards. During the rising phase the loop evolves coherently as a single magnetic tube. The brightness profile is asymmetric with respect to the loop apex at all times; the brightness contrast between the footpoints and the apex decreases with time from a ratio of ~ 10 to ~ 3. After the loop has become all visible, the several parallel filaments which form it follow an independent evolution. Assuming a plasma temperature of ≈ 1 MK, we infer a plasma density of $\sim 6 \times 10^8$ cm^{-3} and a pressure of ~ 0.2 dyne cm^{-2} close to the loop apex at the luminosity maximum. A companion paper is devoted to modeling the rising phase of this event.

Subject headings: Sun: activity, Sun: corona

1. Introduction

X-ray solar observations have invariably shown that the magnetic field has a fundamental role in structuring the corona on scales ranging from the whole Sun to the limit of angular resolution. It has been inferred that the magnetized corona needs to have a filamentary structure (e.g. Rosner et al. 1978a, Litwin and Rosner 1993).

The physical processes occurring on this very small scale influence the dynamics and energetics of the corona. The need to resolve and study the corona down to such scales has determined a vigorous scientific and technological impulse toward the development of solar UV and X-ray telescopes with high spatial and temporal resolution. TRACE is an important step on the way to sub-arcsecond telescopes. It allows a spatial resolution of 1" in the XUV band and, simultaneously, temporal resolution of the order of few seconds.

The high resolution of TRACE should be of help in exploring the key problem of coronal heating. The recognition in the 1970s that the coronal heating mechanism has to be related to the magnetic field has paved the path to proposals of a host of different heating mechanisms, ranging from direct dissipation of magnetic energy to the channeling of waves which dissipate in corona. The issue on heating is far from being settled and we refer to Narain and Ulmscheider (1996) for a detailed account.

Some of the mechanisms proposed so far envision very localized heating mechanisms; understanding their realism, therefore, will benefit from X-ray observations at high angular observations. One of the best known mechanisms is the heating by nano/microflares (Parker 1988) occurring in mini-current sheets ubiquitous in a magnetic field tangled by photospheric footpoints motions.

In any case the high structuring of the X-ray emitting corona tells us that heating mechanisms can hardly act uniformly over all the corona, and that the heating mechanism has to be highly localized. Heat conduction spreads heat along field lines topologically connected with the site of energy release, and gives rise to coronal filamentary structure. Litwin and Rosner (1993) argue that the highly localized heating mechanism in the corona is caused by the spatial intermittency of the magnetic field, and that the most plausible mechanism appears to be magnetic reconnection at the interface between adjacent coronal flux bundles. The time structure of the heating is equally important: any mechanism highly localized in space will, most likely, also be very intermittent in time, giving rise to sequences of heating episodes rather than to a continuous smooth heat release.

Many of the coronal observations, most notably those with Yohkoh and SOHO, have indeed shown a highly dynamic and variable corona. TRACE can provide a better evidence of the intermittency (both spatial and temporal), because of its high angular resolution, its uninterrupted observations and because it is observing in rather narrow spectral bands. Emission in the few lines falling within any such bands, in fact, should be subject to variability, due to variations in plasma temperature as well as density, more easily than broad bands.

A conclusive word on explaining coronal heating mechanisms is still missing, largely because observations have so far placed few constraints on the models: the location and duration of the heating has not been directly observed, also because of the strong effect of thermal conduction and of the thermal inertia of the plasma.

We study a TRACE observation of a solar active region, which monitors the evolution of a highly transient coronal loop. The loop is particularly well defined and identified with respect to the neighboring structures, despite the region being crowded with bright structures. The high cadence (30 s) of the exposures allows us to follow the loop evolution in detail from the very beginning of its brightening.

Previous studies (e.g. Peres et al. 1987, Reale & Peres 1995) have shown that the evolution of the brightness of a loop is related to the heating location and evolution in a complex way: for instance, the region of highest brightness (in the band of the instrument) is not necessarily the location where the heating occurs. What we see is actually the result of folding the plasma brightness with the instrument response. In turn, the plasma brightness is determined by its density and temperature, which depend non linearly from the heating through the dynamic and thermal evolution of the plasma itself.

Since TRACE is a narrow band instrument, and therefore most sensitive to plasma in a relatively narrow range of temperatures, there are non-trivial effects on the detected plasma brightness due merely to the entrance (or exit) of the plasma temperature into (or from) the range of maximum instrument sensitivity. The scenario is further complicated by the effect of plasma thermal conduction which smoothes rapidly any temperature increase along the loop.

The whole project encompasses a detailed morphological analysis of the observed region, in this Paper, and, in Paper II, the hydrodynamic modeling of the loop brightening. We will first study the loop region and its evolution before the loop appears. Attention will then be paid to the loop morphology, geometry and brightness evolution.

This paper, dedicated to the morphology of the event, is structured as follows: in Section 2 we describe the observation, in Section 3 we give a general and qualitative description of the loop region and its evolution, and in Section 4 we analyze quantitatively the loop and derive physical characteristics. In Section 5 we discuss the results.

2. The observation

TRACE (e.g. Tarbell et al. 1994) was launched on a Pegasus launch vehicle on 2 April 1998, from Vandenberg Air Force Base. The telescope has a 30 cm aperture and uses normal-incidence multi-layer mirrors segmented into four quadrants with different coatings. This allows observations in three very narrow ($\lesssim$ 10 Å) XUV bands, centered at 171 Å, 195 Å, 284 Å; the fourth mirror is devoted to a band in the UV. Pointing is internally stabilized to 0.1 arcsec against spacecraft jitter. A 1024×1024 CCD detector collects images over an 8.5×8.5 arcmin field-of-view (FOV).

The TRACE observation of interest for this study was done in the 171 Å band on June 26, 1998. The image sequence starts at 13:01 UT and ends at 15:25 UT, with a total duration of about 8700 s. It includes 213 frames of 1024×1024 pixels, with pixel size 0.5 arcsec, sampled regularly every 30 sec. Fig.1 shows the whole field of view at the initial time. The exposure time of each frame is 23 sec. In the image sequence there are 6 major gaps, which start at 13:11:29 (duration 410 s), at 13:24:47 (450 s), at 13:58:15 (402 s), at 14:43:23 (140 s), at 14:49:12 (568 s), and at 15:01:39 UT (520 s). The center of the field of view is at coordinates X=-492.8" Y=253.9" from the solar center and is fixed during the observation.

The data have been subject to a standard processing. Cosmic ray spikes have been removed from each image and the images have been shifted to a reference system comoving with the solar rotation. A subregion 256×256 pixels ($128" \times 128"$), with lower corner pixel coordinates x=256, y=334 pixels (x=128", y=167") has been selected from the whole field of view.

The main target of our investigation is a loop located in AR 8253, a complex region resolved by TRACE as a multitude of structures on various spatial scales and of different surface brightness. Therefore the loop is among many other loop structures, although it is very well-defined in the images as soon as it appears. We will study the evolution of the loop mainly as a stand-alone structure, but with attention to possible interactions with the nearby structures.

In order to analyze the brightness distribution along the loop and its evolution, we need to correct for the influence of other bright structures lying along the same line of sight, and to subtract background contributions. Given the crowdedness of the region, this operation is indeed non-trivial. We discarded the solution to apply a local background subtraction, i.e. to subtract the average brightness of the region surrounding the loop from the loop brightness itself. A more adequate solution has been to subtract a reference image from all the images, which amounts to a pixel-by-pixel background correction. After an extensive analysis, we have chosen to subtract frame 26 taken at time 13:20:18 UT, because, in this frame, neither the loop, which will appear later, nor other transient structures which cross the loop region at earlier times, are visible.

3. General morphology and evolution

3.1. The whole region

As mentioned above and shown in Fig.1, the total FOV includes a wealth of bright coronal structures on various spatial scales, in addition to a central bright core (*moss*), mainly consisting of small and irregular bright filaments and knots, and highly variable in time. Most of the knots are presumably the footpoints of hot and compact high pressure coronal structures (Peres et al. 1994, Berger et al. 1999, Fletcher & De Pontieu 1999). Large coronal loops, with a total length of the order of 3×10^5 km and more, arise from some of these bright spots; they appear highly structured, and fainter and fainter going from the footpoints to the apex. These large structures appear to be relatively stable and steady during all the observation. Many other loop structures are clearly visible in all the images.

3.2. The initial evolution

We will now describe qualitatively the evolution of the loop and of the surrounding region.

We concentrate on the central 256×256 subregion outlined above, which includes the loop of interest. Fig.2 shows a sequence of frames during the evolution of the region[1]. Some of them (from frame 37 to 85) are background subtracted, in order to follow better the loop evolution in the rising phase. An accompanying sketch (Fig.3) defines the bright structures we shall refer to, superposed on a relevant magnetogram collected between 13:35 and 14:30 UT.

The initial frame (13:01 UT, frame 0 in Fig. 2) shows bright irregular patches on the right (eastern) side (region **A**) with a thin and long ($\approx$ 100" $\times$ 25") extension, crossing diagonally the center of the region from north-east to south-west. The western side of the frame is darker and shows several thin loop segments. Two of them, L_1 and L_2 , seem to run approximately parallel to each other, with the apex to the south and an apparent length of about 3×10^9 cm each: L_1, the northern one, shows only the left leg, and L_2 quite a straight right leg. These two loops, and in particular L_2, undergo a very dynamic evolution during the first part of the observation: a bright blob on the right leg of L_2 (albeit not very evident in the initial frame) travels clockwise along the loop and, at the same time, brightens, reaching its maximum brightness at about 13:08 UT ($t \sim 400$ s after the beginning, see frames 6 and 12), i.e. when it is approximately at the loop apex.

While the blob moves in the L_2 eastern leg, a third loop brightens, L_3, whose western leg is adjacent to L_2 eastern leg. L_3 is best visible at 13:05 UT (frame 12). A minor bright front in L_3 moves together with the major blob in L_2. When the blob, or brightening, reaches the point where L_2 and L_3 diverge, it bifurcates between the two and then continues to travel separately along the legs of both loops.

At 13:11 UT ($t \sim 600$ s) the blob is in the other leg of L_2 and at 13:21 UT ($t \sim 1200$ s, frame 28) it has reached its far end, while L_3 has practically disappeared, leaving just some irregular structures at the site of its divergence from L_2. These irregular structures appear as a relatively bright bundle of short filaments; we will call it structure **B**. Structure B has a size of $\sim$ 15" and is steadily bright for all the remaining observation time, although both its structure and luminosity are highly variable. On the contrary, L_1 and L_2 gradually disappear and are no longer visible after $\sim$ 1 hour since the beginning of the observation.

The blob takes about 1300 sec to travel along a projected length of $\sim 3 \times 10^9$ cm with an apparent average speed of $\sim$ 25 km/s. Due to possible projection effects this is a lower limit to the blob speed, assuming it is due to moving material. For a plasma at $\sim$ 1 MK, the temperature of maximum sensitivity in the TRACE 171 Å band, this is well below the sound speed ($\sim$ 100 km/s). From the analysis of the blob close to its maximum brightness (at 13:06 UT), its radius can be estimated to be $\approx$ 9 pixels, corresponding to a volume $\approx 1.3 \times 10^{26}$ cm^3, if it is roughly spherical. If its temperature is $\sim$ 1 MK, from the luminosity integrated in the blob we estimate an emission measure 4×10^{44} cm^{-3} and a density $\approx 2 \times 10^9$ cm^{-3}. The synchronous motion of bright blobs in loops L_2 and L_3 suggest that these two loops may interact.

3.3. The turn–on of loop L_4

The loop that we study, outlined in frame 28, is different from all the others discussed so far and is not yet visible when the blob has completed its travel along L_2 and L_3 . It is larger than the previously described loop structures and its apparent orientation is similar to that of loops L_1 and L_2 . The details of the geometry of the loop, which we will call loop L_4 , will be illustrated in section 4.1.

The loop footpoints brighten first. From the inspection of the background subtracted images we see that at $t \simeq 1900$ s (13:32 UT, see frame 37) the footpoints become steadily brighter than they were at the beginning of the observation. Later the northern leg brightens, from the footpoint up toward the apex. With a delay of approximately 2-3 minutes, also the southern leg begins to brighten faintly. As soon as it begins to brighten, this leg seems to diverge into two separated footpoints (they may be two overlapping loops). The southern branch, however, is quite faint and disappears completely at 14:05 UT. As shown by the sequence of background subtracted images in Fig.2, at 13:39 UT ($t \sim 2300$ s, frame 51) the loop is entirely visible although the apex and the southern leg are still very faint. At 13:42 UT ($t \sim 2500$ s, frame 57) a very bright front rises from the northern footpoint and at 13:49 UT ($t \sim 2900$ s, frame 71)

[1] An animation of the sequence is available at http://www.astropa.unipa.it/....

a less conspicuous one from the southern footpoint. These two fronts join in the southern leg at 13:56 UT ($t \sim 3300$ s, frame 85): the whole loop is much brighter than the adjacent structures. The apparent speed of the brightness fronts is of the order of 100 km/s (without correction for the angle of the plane of the loop with the solar surface).

Note that the loop crosses structure B in the image: an interaction between the two structures is possible although a chance coalignment cannot be excluded.

3.4. The decay of loop L_4

After $t \sim 3300$ s, while the evolution of the overall loop brightness is more gradual, the morphology becomes more complex, because it becomes evident that it is structured in several parallel filaments (at least 4 bright and 3 dark) which follow slightly different evolutions. Further outer filaments progressively brighten and make the whole structure wider and wider giving the appearance of an outward expansion. At the same time the northern footpoint begins to fade away. At 14:15 UT ($t \sim 4500$ s) a distinct outer loop begins to appear. This loop is fainter than L_4 and reaches its maximum luminosity at 15:15 UT ($t \sim 8000$ s, frame 192). At 15:00 ($t \sim 7100$ s, frame 176) L_4 is clearly into its decay phase: its apparent width decreases because less and less filaments are visible. At the final time 15:25 UT ($t = 8653$ s, frame 212) it is still clearly visible although fainter than before.

4. The loop morphology and characteristics

4.1. The geometry of loop L_4

As mentioned before, L_4 is larger than loops L_1 , L_2 and L_3, and its orientation is similar to that of L_1 and L_2 . Its footpoints are located in moss regions full of irregular structures, which are probably the footpoints of other, hotter, coronal arches (Peres et al. 1994, Di Matteo et al. 1999, Berger et al. 1999, Fletcher & De Pontieu 1999). The northern footpoint (position X=186", Y=265") lies northward of region A, while the southern one (X=218", Y=215") is close to the footpoints of much bigger arches.

The distance d_{foot} between the two footpoints of L_4 , taking into account the effect of the solar surface curvature (5%), is $\approx 4.3 \times 10^9$ cm. The projected distance d_{apex} of the loop apex from the line joining the footpoints is also $\approx 4 \times 10^9$ cm. If the loop were semicircular, d_{foot} would be the loop diameter and the distance d_{apex} should be less than the loop radius (allowing for an arbitrary tilt of the plane of the loop over the solar surface), i.e. $d_{foot}/2$, while the total loop length would be $L = \pi d_{foot}/2 \approx 7 \times 10^9$ cm. The apparent length measured along the loop is, instead, $L \approx 1.0 \times 10^{10}$ cm, i.e. 40% longer. Therefore the loop is not semicircular, but elongated. This elongation cannot be due to projection effects which would, instead, cause an apparent "shortening" of the arch.

The loop shape appears very regular and symmetric as if it were seen on a front view. The loop lies well within the solar disk, and, if it rose vertical from the solar surface, significant projection effects would be expected: the loop should appear more squashed than it really appears, and the real total length would be $\sim 2 \times 10^{10}$ cm, i.e. twice the apparent length and three times the length derived from the footpoints distance if it were semicircular. Such a loop would be rather stretched and difficult to explain.

It is much more likely that *the loop is significantly inclined with respect to the vertical to the solar surface.* On the other hand the loop cannot be completely horizontal on the surface, since in this case it would be initially filled up with chromospheric material, both because of being very close to the chromosphere, and because it would extend over a very small fraction of the vertical density scale height. As shown in Paper II, under these conditions any additional heating would make loop regions far from the footpoints brighten first, just because of the temperature increase. This is not observed. The observed fronts moving from the footpoints require instead a significant rise of plasma from the footpoints, which is possible only if the loop is initially "empty".

We conclude that the loop is, quite likely, inclined relative to the surface at an intermediate angle. An inclination of $\approx 60°$ with respect to the vertical is a good compromise to obtain both reasonable loop geometry and stratification[2].

This implies that the total loop length is close to that estimated directly on the images, i.e. 1.0×10^{10} cm, or longer by no more than 15%. The maximum height of this loop above the surface $\sim 2 \times 10^9$ cm is significantly lower than the pressure scale height at 1 MK ($\sim 5 \times 10^9$ cm). Therefore if the loop were

[2]Indeed this configuration produces the best results for modeling, as described in Paper II.

in hydrostatic conditions at 1 MK, it would be filled with a significant amount of coronal plasma.

The loop geometry does not change substantially during the entire time the loop is visible. Only near the end of the observation, we observe that the inner filaments which compose the loop rapidly fade away while the outer ones stay bright for a longer time; the visual impression is, therefore, that the loop seems to enlarge (see Sect.3.4).

4.2. The plasma physical conditions in loop L_4

For an insight into the physical conditions of the plasma inside the loop, we analyze the loop conditions close to its maximum luminosity, when the signal-to-noise ratio is high and the plasma density is presumably at maximum. In particular, we consider a frame at 14:16 UT. As we will see in the following, the loop total luminosity is almost constant near the maximum for a time longer than the loop thermal decay time (assuming $T \sim 1$ MK), and for that time we can consider the loop as steady for our analysis. We then assume that, when the loop is at maximum luminosity, the temperature of the emitting plasma far from the footpoints is around the temperature of maximum sensitivity of the 171 Å filter, i.e. $T \sim 1$ MK.

At this time, the loop FWHM cross section diameter is ≈ 18 pixels (9"), as deduced from the transversal brightness profile measured at a point between the northern footpoint and the apex. In order to estimate the plasma density, we then consider a strip 18 pixels wide along the loop longitudinal axis, and take a section of the strip 10 pixels (5") long at a distance of $\sim 4 \times 10^9$ cm from the northern footpoint, close to the loop apex. The total detected luminosity of this section is ≈ 260 DN/s. If we assume an emissivity of $\approx 9 \times 10^{-27}$ DN/s/pixel per unit emission measure in the instrument band, we obtain an emission measure of 4×10^{43} cm^{-3}. If we consider this section as a part of a long cylinder of radius 9 pixels, its volume is 1.1×10^{26} cm^3, yielding an average density of $\sim 6 \times 10^8$ cm^{-3} and a pressure of ~ 0.2 dyne cm^{-2} at 1 MK. These values are not unusual for relatively long active region loops. The density value can be considered a lower limit which could increase should the plasma temperature be lower or higher than 10^6 K, because the filtered emission per unit emission measure would be significantly lower.

If we apply the scaling laws of Rosner et al. (1978b) to a loop of pressure 0.2 dyne cm^{-2} and a semilength of 5×10^9 cm, we obtain a loop *maximum* temperature of $\sim 1.4 \times 10^6$ K. The resulting slight inconsistency can be due, in part, to the loop maximum temperature being slightly higher than the estimated "filtered" temperature, or, more likely, shows that the loop never reaches conditions of complete equilibrium during the observation.

4.3. The brightness distribution in L_4 and its evolution

We now analyze more in detail the distribution and the evolution of the plasma emission along the loop. To this aim, we extract the emission of all pixels along the loop from each background-subtracted image. As shown in Fig.4, on a frame where the loop is very luminous, we draw a path along the loop, following the locus of the brightest points; then we consider a strip of constant width along the loop and centered on this path, and the strip is divided into sections of equal length (e.g. 10 pixels). The brightness is averaged in each section, in order to obtain the brightness distribution along the loop, and, at the same time, to achieve a higher statistical significance and to reduce the noise. This analysis is analogous to that applied to loop structures observed with NIXT by Di Matteo et al. (1999). The strip is kept fixed for the entire image sequence: this causes slight fluctuations of each sector brightness, due to imperfect correction for solar rotation.

Fig.5 shows the background subtracted loop light curve integrated on a strip 10 pixels wide and binned on 200 sec time intervals. We have verified that the light curve does not change much by taking thinner strips down to 4 pixels wide. The light curve first rises for the presence of the blob crossing the loop region before the loop becomes visible. Then we have the loop rise phase proper: the total loop luminosity increases by more than one order of magnitude with an e- folding rise time of ~ 800 sec, which is of the same order as the isothermal sound crossing time at 1 MK. The luminosity is maximum at 13:58 UT, almost an hour after the beginning of the observation and ~ 1600 sec after the loop first appears; the loop brightness remains almost steady, with a slight decrease, for the next hour. The e-folding decay time in this phase is ~ 14000 sec. Then, after a data gap, there is a significant jump to lower values and the decay becomes faster, with a decay time ~ 6000 sec. The jump is due to the rapid disappearance of the brightest loop filament, around which the path has been constructed; most of the loop emission then comes from an outer region, part of which falls outside the strip (see Fig.2c, frame 212), tailored to study at best the initial phases of the evolution.

We now examine the loop rising phase more closely. This is in fact the phase in which the brightness evolves coherently across the loop, i.e. the loop behaves as a single loop filament.

From inspection of the light curves of different sectors along the loop we notice that the loop apex begins to brighten $\sim$ 500 sec after the footpoints, due to the presence of the moving brightness fronts. The e-folding rise time is longer at the southern footpoint ($\sim$ 1100 s) than elsewhere ($\sim 600 - 800$ sec), showing that the evolution is not symmetric and that the brightness contrast between the apex and the southern footpoint decreases during the rising phase.

This behavior emerges more clearly from the brightness profiles along the loop. The profiles shown in Fig.6 are taken in a four pixels (2") wide strip along the loop, by averaging the brightness in sectors 10 pixels (5") long, and have further been smoothed with a boxcar 3 sectors wide.

At the beginning of the rising phase (time = 1875 s) only the footpoints are visible and there is a significant count excess at $\approx 3 \times 10^9$ cm from the southern footpoint, where the remnant of the blob is (structure B, see Section 3.2). After $\sim$ 500 sec the brightness profile has all significantly increased and the enhancement continues steadily still for about 1000 sec, amounting, at maximum, to a factor $\sim$ 10 at the loop center and to $\lesssim 5$ at the footpoints. The southern footpoint brightens less than the other regions, i.e. by only a factor $\sim$ 4. The brightness contrast between the footpoints and the apex is higher at the beginning ($\gtrsim 10$) and decreases to ~ 3 at $t \simeq 3400$ s. Indeed, the contrast that we measure at the beginning is a lower limit because the background signal is significant in the faint loop center.

The count excess corresponding to structure B progressively reduces as the loop brightens, and is negligible for $t > 3000$ s. The brightness does not rise always uniformly: most noticeably, the brightness profile on the right (northern) leg is steeper at the beginning than at the end of the rising phase.

Around the time of maximum luminosity ($\sim$ 3400 s) the brightness distribution appears asymmetric: the northern footpoint is brighter than the southern one, and the brightness gradient is higher in the northern leg. This asymmetry and the brightness contrast footpoint/apex tend to decrease later (see profile at time 4044 s). In particular the northern footpoint begins to decay, earlier and faster than the other regions.

After this phase, the evolution of the loop brightness becomes more complex and difficult because of the different evolution of the filaments which compose the loop. The structure and the evolution of the loop filamentation is a very interesting topic but is outside the scope of this work. It deserves a very accurate and detailed study by itself.

5. Discussion and conclusions

This work is devoted to the presentation and analysis of the morphology and evolution of a loop (and its surrounding region) whose progressive brightening has been monitored by TRACE with unprecedented detail.

The description and analysis presented above show that the region object of the present study is very complex and dynamic. In particular, there is evidence of plasma motion (the blob), of changes of the local coronal structure, and of the appearance of a well-identified coronal loop (L_4), whose brightness evolves. This observation is important in many aspects:

- the spatial resolution is unprecedented;
- a highly transient loop brightening is monitored, with good coverage and time resolution;
- the loop is monitored since its early brightening;
- the geometry of the loop does not change substantially during the observation;
- the temporal cadence is high and constant, allowing us to analyze clearly the evolution of the transient brightness distribution along the loop.

The loop is a relatively long active-region loop, probably slanted on the surface and rather elongated. We may in general interpret its evolution in terms of an initially empty and cool magnetic flux tube which is filled up of coronal plasma due to a transient heating episode occurring somewhere along it.

In spite of the high quality of the observation and of the well-defined loop evolution, the physical interpretation of the data is by no means trivial because many concurrent effects determine how the loop evolution is detected by the telescope. Modeling this phenomenon, and in particular the loop rising phase, is the task of Paper II.

Unfortunately, since the data are available in a single filter band, direct plasma temperature diagnostic is missing. However, in this specific case, this may be considered a relatively minor problem, since, as shown in section 4.2, the narrow spectral band, and the high sensitivity to plasma temperature around 1 MK, allows us to constrain the plasma physical conditions.

For the purpose of physical interpretation, it is also very important to note that there is a well-identified phase, the rising phase, in which the loop brightness evolves with a high degree of coherence, such that even moving fronts can be identified. This coherence allows us to describe the loop as a single structure in the rising phase, both here and in Paper II. Moreover we notice that this coherent evolution has, by itself, important implications: the initial heating which ignites the loop must be deposited across a large fraction of the loop cross section simultaneously. This is no longer true later, when it appears clear that the several loop filaments which form the loop follow independent evolution. This makes it difficult to treat the loop as a single structure at later times. On the other hand it is in principle possible to analyze the transverse structure of the loop, an important topic in coronal physics.

The other important characteristic of loop L_4 is that it is highly transient. Even when the light curve is almost steady, the individual filaments are highly variable. This may suggest that, late during the evolution, on the average, the heating rate is almost constant, but other features, such as the heat source position across the loop, vary continuously.

Before it brightens, the loop region is the site of highly dynamic events: a bright blob travels along the common leg of two adjacent loops and then bifurcates, the largest part ending at the northern leg on one of the two loops. Such an evolution may suggest the occurrence of a transient energy release due to reconnective processes in a localized region, maybe tied to the loop ignition. Fig.3 emphasizes the apparent spatial closeness of the structures which may suggest their possible interaction. The magnetogram clearly shows that the northern and southern footpoints of loop L_4 are located in photospheric regions of negative and positive magnetic field polarity, respectively, with an intensity of the longitudinal component between 100 and 200 G.

At its maximum luminosity the loop is a very bright structure, probably because it is filled with plasma at a temperature not far from the temperature of maximum sensitivity in the TRACE 171 Å band. The footpoints are brighter than the apex at any time, and the northern one is also the brighter of the two. This characteristic is typical of bright loops, as detected by narrow band X-ray telescopes mostly sensitive to relatively cold ($\sim 10^6$ K) lines, as is also NIXT (Peres et al. 1994). However the contrast between the footpoints and the apex is lower than that expected from hydrostatic modeling (see Paper II), suggesting that the loop never really reaches steady and hydrostatic conditions. Furthermore, the brightness distribution is not symmetric, suggesting a non-symmetric heating deposition and evolution.

At this stage of the analysis we cannot put any other constraint on the heating source. Naively, one may think heating to be located close to the northern footpoint, the first to brighten and also the brightest loop region. On the other hand, if one looks globally at the loop evolution, it may appear as relatively gradual and uniform and may even suggest a rather uniform heating. The following questions are then in order: What agent heats and turn the loop on? Does it have any connection with the initial dynamic loop interaction? Is there any hint of an impulsive turn on of the heating? Is the heating steady afterwards? Is there any connection with the very dynamic evolution observed in the region before the loop begins to brighten? We will try to answer these and other questions in Paper II with the aid of a hydrodynamic loop model.

FR, GP and SS acknowledge support from Ministero della Ricerca Scientifica e Tecnologica and from Agenzia Spaziale Italiana. EED and LG were supported by Contract No. NAS5-38099 from NASA to LMATC. We thank Ms. R.A. McMullen for assistance with the data analysis and with mission operations.

REFERENCES

Berger, T.E., De Pontieu B., Schrijver, C. J., & Title, A. M., 1999, ApJL, 519, L97.

Di Matteo, V., Reale, F., Peres, G., & Golub, L., 1999, A&A, 342, 563.

Fletcher, L., & De Pontieu B., 1999, ApJL, 520, L135.

Litwin, C., & Rosner, R., 1993, ApJ, 412, 375.

Narain, U., Ulmschneider P., 1996, Space Science Rev., 75, 453.

Parker, E. N., 1988, ApJ, 330, 474

Peres, G., Reale, F., Serio, S., Pallavicini, R., 1987, ApJ, 312, 895.

Peres, G., Reale, F., & Golub, L. , 1994, ApJ, 422, 412

Reale, F., Peres, G., 1995, A&A, 299, 225.

Reale, F., Peres, G., Betta, R., DeLuca, E.E., Golub, L., 1999, ApJ, submitted (Paper II).

Rosner, R., Golub, L., Coppi, B., Vaiana, G. S., 1978a, ApJ, 222, 317.

Rosner, R., Tucker, W., Vaiana, G.S., 1978b, ApJ, 220, 643.

Tarbell T. D., et al. 1994, in Proc. of the Third SOHO workshop - Solar Dynamic Phenomena and Solar Wind Consequences, 26-29 September 1994.

This 2-column preprint was prepared with the AAS LATEX macros v4.0.

Fig. 1.— Total field of view of the TRACE (171 Å band) observation. The frame is made of 1024 × 1024 square pixels of size 0.5", taken at 13:54:17 UT, 3195 sec since the beginning of the sequence. The exposure time is 23 sec and the brightness scale units are Digital Numbers (DN). The square encloses the subregion, shown in Fig.2, containing the loop which we study. The arrow indicates the loop which is the main focus of this analysis.

Fig. 2.— Selected frames during the evolution of the target region from the beginning to the end of the TRACE observation. The time is reckoned since the beginning of the observation sequence. The grey scales are in units of DN. Regions A and B and loops L_1 , L_2 and L_3 are marked. On frame 28 and 37 the loop is outlined. Frame 26 has been subtracted from frames 37 to 85, to emphasize the loop evolution. The arrows indicate the bright moving blob in frames 0 to 22, the loop footpoints in frame 37, the brightness fronts moving from footpoints in frames 57 and 71, and the outside concentric loop in frame 192 (see text).

Fig. 3.— Sketch (in scale) of the main structures involved in the transient phenomena described in this Paper, superposed on a magnetogram taken at Kitt Peak Solar Observatory between 13:35 and 14:30 UT. The magnetic field intensity is in Gauss, and white is positive polarity.

Fig. 4.— Strips as the one shown (this is 10 pixels wide) have been used to analyze the brightness along the loop. Each strip is, in turn, divided into equal-length sections (20 pixels long, in this case), over which the pixel brightness is averaged. The image is taken at 13:54:17 UT (frame 80).

Fig. 5.— Light curve of the whole loop in the TRACE 171 Å band. The flux is background-subtracted and integrated along a strip 10 pixels wide, as shown in Fig.4, and on 200 sec time intervals; the time is reckoned since the beginning of the observation.

Fig. 6.— Distributions of brightness along the loop at various times (measured in seconds since the beginning of the observations); approximately up to the beginning of the decay phase. The coordinate along the loop is reckoned from the southern footpoint.

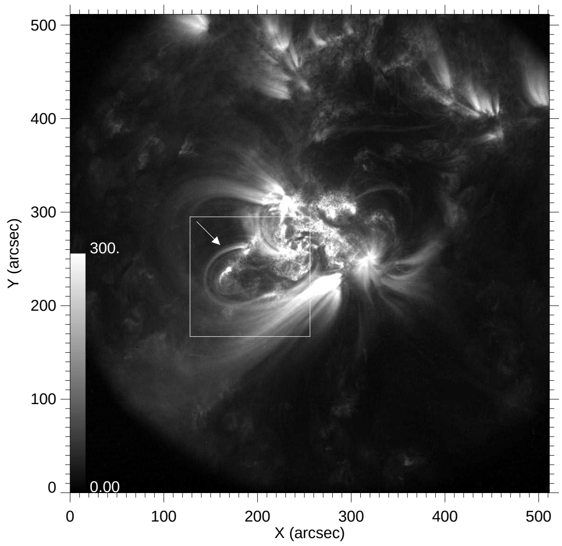

Fig. 1.—

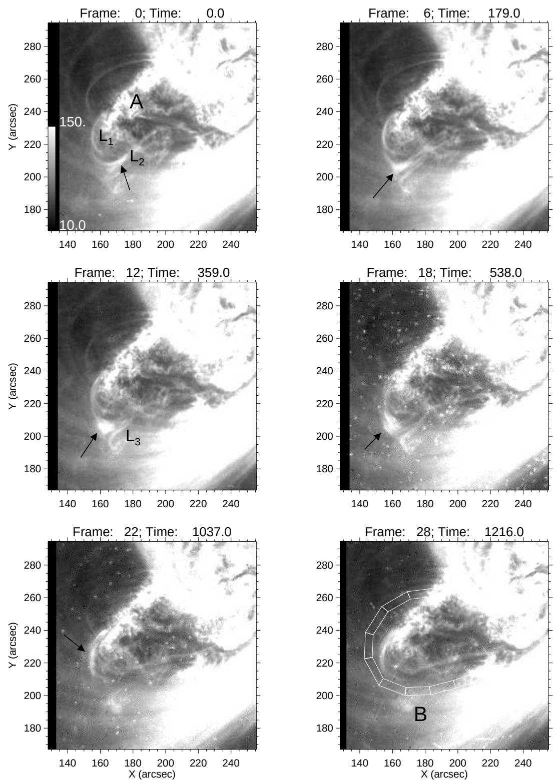

Fig. 2a.—

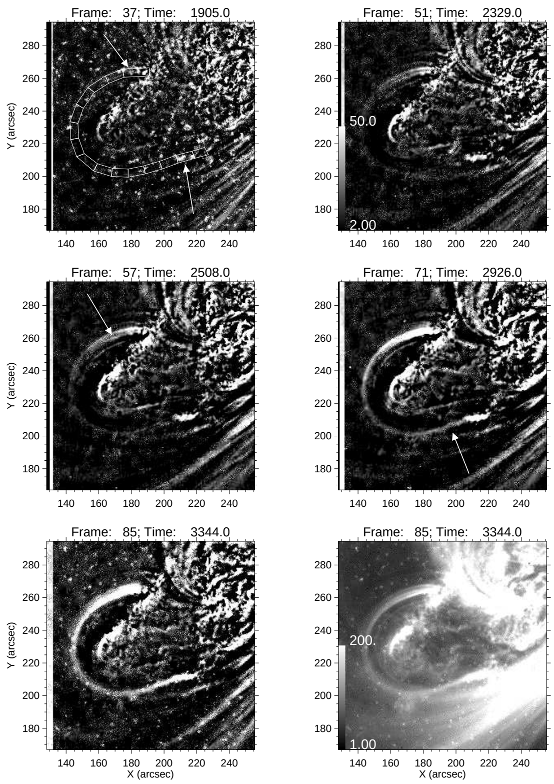

Fig. 2b.—

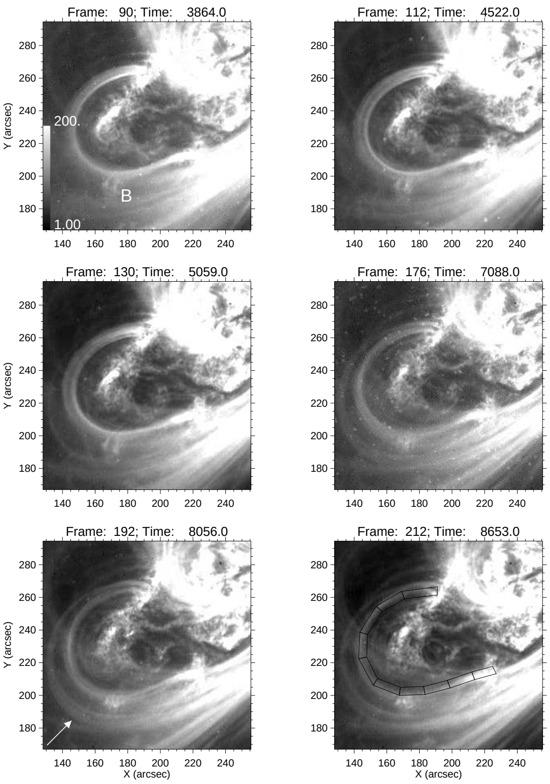

Fig. 2c.—

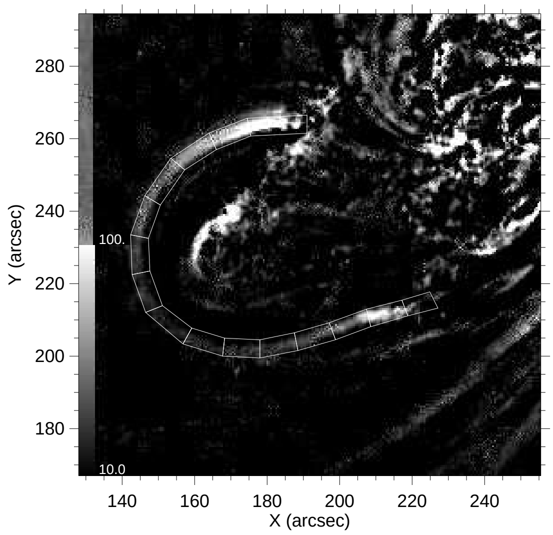

Fig. 4.—

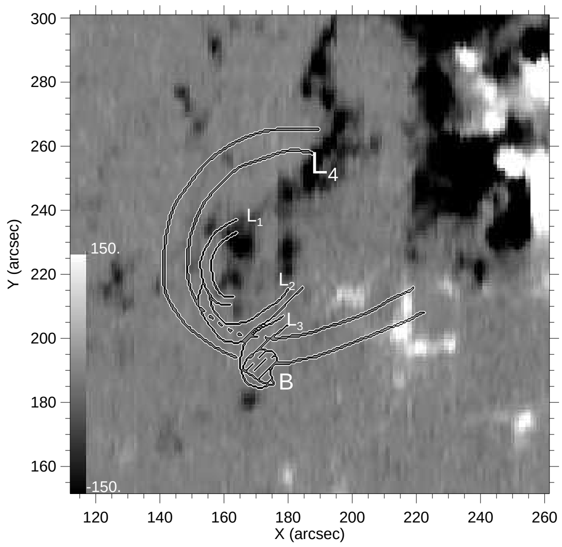

Fig. 3.—

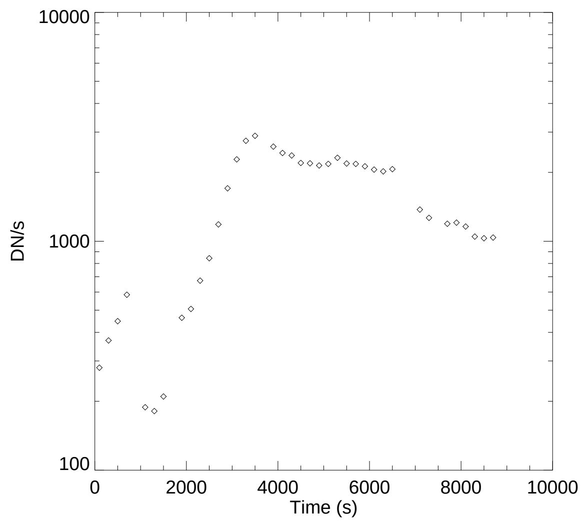

Fig. 5.—

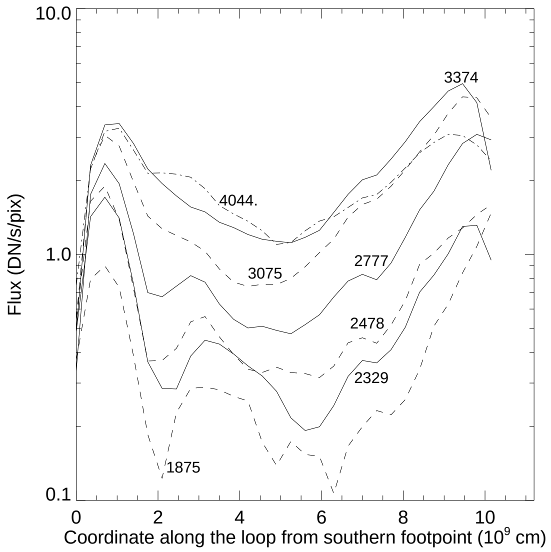

10.0
1.0
0.1
Flux (DN/s/pix)
0
2
4
6
8
10
Coordinate along the loop from southern footpoint (10^9 cm)
3374
4044.
3075
2777
2478
2329
1875

Fig. 6.—